

Two-qubit conditional quantum-logic operation in a single self-assembled quantum dot

S. J. Boyle,^{1,*} A. J. Ramsay,^{1,†} F. Bello,¹ H. Y. Liu,² M. Hopkinson,² A. M. Fox,¹ and M. S. Skolnick¹

¹*Department of Physics and Astronomy, University of Sheffield, Sheffield S3 7RH, United Kingdom*

²*Department of Electronic and Electrical Engineering, University of Sheffield, Sheffield S1 3JD, United Kingdom*

(Received 20 May 2008; published 1 August 2008)

The four-level exciton/biexciton system of a single semiconductor quantum dot acts as a two-qubit register. We experimentally demonstrate an exciton-biexciton Rabi rotation conditional on the initial exciton spin in a single InGaAs/GaAs dot. This forms the basis of an optically gated two-qubit controlled rotation (CROT) quantum-logic operation where an arbitrary exciton spin is selected as the target qubit using the polarization of the control laser.

DOI: [10.1103/PhysRevB.78.075301](https://doi.org/10.1103/PhysRevB.78.075301)

PACS number(s): 78.67.Hc, 03.67.Lx, 42.50.Hz, 78.47.jp

I. INTRODUCTION

Two-qubit gates that operate on a “target” qubit conditional on the state of the “control” qubit, such as the controlled rotation (CROT) gate, provide the basic tool for entangling and disentangling qubits and are therefore a critical component of any quantum processor.¹ One possible realization of a quantum processor is based on the use of semiconductor quantum dots (QDs), where the qubit is encoded in the presence or absence of an exciton and manipulated using picosecond laser pulses. To date, considerable experimental progress has been made in the coherent optical control of a single exciton qubit,^{2–5} and a two-qubit gate has been reported for two excitonic qubits hosted in a single GaAs interface dot.⁶ In the latter case, a CROT gate is realized by driving a Rabi rotation on the exciton-biexciton transition, similar to proposals in Refs. 7 and 8

With respect to potential applications in quantum information, InAs-based self-assembled dots have several advantages over GaAs interface dots. For example, InGaAs dots have longer coherence times⁹ and greater control over the growth process, enabling coupled dot structures^{10,11} and positioning of dots¹² (both of which offer potential for scalability). In spite of this potential there have been no experimental studies of the control of two-qubit systems in self-assembled dots.

Here we report on the conditional coherent optical control of two exciton qubits hosted in a single InGaAs/GaAs quantum dot. This is achieved by observing an exciton-biexciton Rabi rotation conditional on the initial state of the exciton spin, where the π pulse acts as a CROT gate. In contrast to Ref. 6, we investigate the case of a CROT gate where the polarization of the control laser is used to address both exciton-biexciton transitions simultaneously. In similar atomic systems arranged in a three-level Λ configuration, when two lasers are used to address each transition, arbitrary superpositions of the lower-energy states can be coupled to the upper state.¹³ In a quantum dot context, this provides a potential tool for selecting arbitrary exciton spin superpositions as the target and control qubits, providing a degree of control over the two-qubit operation.

II. EXPERIMENT DETAILS

The experiments are performed on a single quantum dot embedded in an n - i Schottky diode structure. The wafer is

consists of a GaAs substrate with the following layers deposited by molecular-beam epitaxy: 50-nm n^+ doped GaAs, 25-nm i -GaAs spacer, a single layer of low-density InGaAs dots ($30\text{--}60\ \mu\text{m}^{-2}$), a further 125-nm i -GaAs spacer, a 75-nm $\text{Al}_{0.3}\text{Ga}_{0.7}\text{As}$ blocking barrier, and a 5-nm i -GaAs capping layer. The wafer is processed into ($400 \times 200\ \mu\text{m}$) mesas with a semitransparent titanium top contact and an aluminum shadow mask patterned with 400-nm apertures using e-beam lithography to spatially isolate single dots. At low temperatures ($T \sim 10\ \text{K}$), the dark current of the photodiode in reverse bias is instrument limited for all voltages of interest: ($\Delta I_{\text{rms}} < 50\ \text{fA}$ and $I_{\text{offset}} < 200\ \text{fA}$ for at least $V_{\text{reverse}} < 5\ \text{V}$).

The experiments described here employ a sequence of two spectrally narrow synchronized laser pulses with independently tunable wavelengths and time delay. Figure 1 shows an illustration of the optics used to generate this pulse sequence. A mode-locked Ti:sapphire laser provides a source of 150-fs pulses with a repetition rate of 76 MHz and a

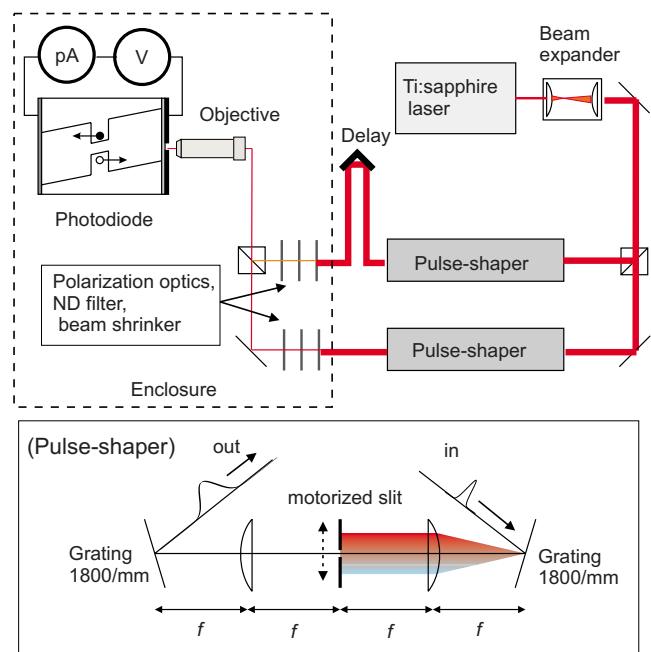


FIG. 1. (Color online) Schematic diagram of the experimental setup with close up of the pulse shaper.

center wavelength tuned to 951 nm. The beam is collimated and expanded before being split using a polarizing beam splitter to control the amount of power in each arm. A $4f$ zero dispersion pulse shaper¹⁴ is placed in each arm and an adjustable slit mounted on a motorized stage is used to filter the spectrally narrow pulses from the spectrally broad input pulse. The spectrum of the resulting laser pulses are a convolution of a rectangle (due to the slit) and a Gaussian (due to diffraction): in these experiments the pulse spectrum has a Gaussian shape with a full width half maximum (FWHM) of 0.2 meV. A delay stage in one arm introduces a time delay between the pulses. The beam diameters are reduced for a more precise control of the power using a motorized variable neutral density filter. The beams are recombined and focused onto the sample with an estimated spot size of $1.2 \mu\text{m}$, using a long working distance microscope objective with a numerical aperture of 0.55. The objective is mounted on an xyz stage with both manual and piezoelectric control in a standard micro-PL arrangement. The sample is held in a cold finger cryostat and is connected to a simple measurement circuit. The circuit consists of a commercially available ammeter (Keithley 6485) and voltage source (Keithley 230) that are connected using standard coaxial cables with careful shielding and avoidance of ground loops. The sample temperature is 10 K.

A photocurrent detection technique is used³ to measure a quasiabsorption spectrum. In this technique, a laser in resonance with an exciton transition creates an electron-hole pair in the dot, which under the action of an applied electric-field tunnels from the dot resulting in a photocurrent proportional to a weighted sum of the final exciton and biexciton populations. Photocurrent detection provides a quantitative and efficient measurement of the final exciton population with a maximum current of one electron per pulse (12.18 pA) corresponding to an exciton population of one. In practice, the detection efficiency is limited by competition with radiative recombination and a hole tunneling rate that can be slow compared to the repetition rate of the laser.¹⁵ The use of a two color excitation scheme enables the study of conditional transitions such as the (X^0-2X^0) and $(h-X^+)$,¹⁶ in addition to the neutral exciton $(0-X^0)$ (Ref. 3) and two-photon biexciton $(0-2X^0)$ (Ref. 17) transitions observed in single color excitation schemes.

III. PRINCIPLE OF OPERATION

The QD exciton-biexciton system may be considered as two excitonic qubits labeled by their spin states. There are four states: the ground state $|00\rangle$, two orthogonally polarized single exciton states $|01\rangle$ and $|10\rangle$, and the biexciton state $|11\rangle$, as illustrated in Fig. 2. The electron-hole exchange interaction causes the energy eigenstates of the exciton to be linearly polarized along the crystal lattice axes, designated as the x and y axes. This results in strong selection rules for linear polarization and a fine-structure splitting of 10–100 μeV . Due to the Coulomb interaction, the ground state to exciton $(0-X^0)$ and the exciton to biexciton (X^0-2X^0) transitions are separated by a biexciton binding energy $\hbar\delta_B$ of a few millielectron volt. The CROT operation

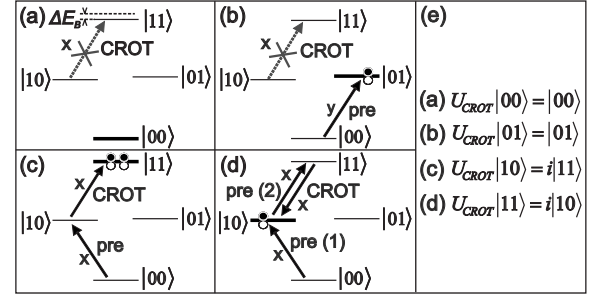


FIG. 2. Implementation of a CROT gate on two exciton based qubits. The QD ground state $|00\rangle$, the two orthogonally polarized exciton (X^0) states $|01\rangle$, $|10\rangle$, the biexciton ($2X^0$) state $|11\rangle$, and the biexciton binding energy ΔE_B are indicated. The CROT operation is performed by an x -polarized π -pulse in resonance with the X^0-2X^0 transition. Cases (a)–(d) show the CROT operation on all four pure qubit states. (e) The CROT truth table.

flips the target qubit if the control qubit is in the $|1\rangle$ state, according to the truth table shown in Fig. 2(e). The gate can be realized by an x -polarized pulse with a pulse area of π in resonance with the X^0-2X^0 transition, labeled as the CROT pulse.

The effect of the CROT pulse on all four pure qubit states is shown in Figs. 2(a)–2(d). (a) The dot is initially in the ground state $|00\rangle$. Hence the CROT pulse is not in resonance with any available transition and is not absorbed. (b) A y -polarized preparation pulse (prepulse) with a pulse area of π —in resonance with the $0-X^0$ transition—precedes the CROT pulse, preparing the y -polarized exciton state $|01\rangle$. The CROT pulse is not absorbed due to polarization selection rules. (c) An x -polarized prepulse prepares the x -polarized exciton state $|10\rangle$ and the CROT pulse excites the $|10\rangle \leftrightarrow |11\rangle$ transition. (d) Having prepared the $|11\rangle$ state as in (c) using the first half of a 2π pulse, the second half of the pulse drives the system back to $|10\rangle$.

IV. CROT GATE

Single-pulse and two-pulse measurements are made on a single QD with a $0-X^0$ transition energy of 1.302 eV at a reverse bias of 0.6 V. In all measurements, “prepulse” refers to a π pulse in resonance with the $0-X^0$ transition. The spectra in Fig. 3 show photocurrent as a function of the detuning with respect to the $0-X^0$ transition of a π pulse. (a) The single-pulse measurement shows the $0-X^0$ transition. Two weak features, labeled as B and C, are also observed due to the excitation of other nearby QDs.¹⁸ (b)–(c) For two-color measurements, this pulse is preceded by the prepulse—which prepares an exciton state. Both pulses are linearly polarized along the crystal axes. (b) In the case of copolarized pulses, an additional peak corresponding to the X^0-2X^0 transition is observed at a detuning of $\hbar\delta_B = -2.41 \text{ meV}$.¹⁹ At zero detuning a dip is observed as the two pulses act as a 2π Rabi rotation; first creating an exciton and then returning the dot to the ground state. (c) For cross polarized pulses, polarization selection rules suppress the X^0-2X^0 transition.

To demonstrate the truth table of the CROT operation, we measure the X^0-2X^0 Rabi rotation for all four pure qubit

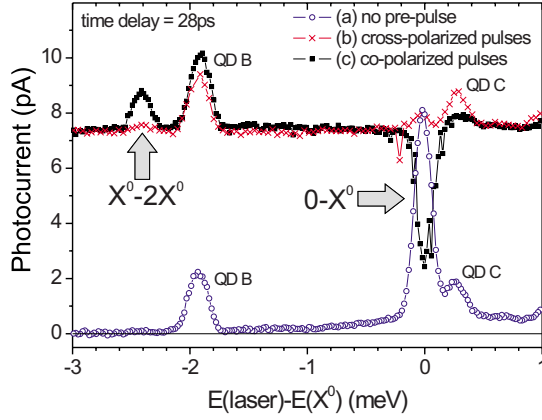


FIG. 3. (Color online) Photocurrent spectra. (○) The single-pulse measurement shows the ground state to exciton transition ($0-X^0$) and two features from neighboring dots (QD B and QD C). For two-pulse measurements, a linearly polarized preparation pulse prepares the exciton state. (■) With copolarized pulses, the exciton-biexciton transition (X^0-2X^0) and quenching of the exciton are observed. (×) With cross polarized pulses the (X^0-2X^0) transition is suppressed by polarization selection rules.

input states. Conditional Rabi rotation measurements are shown in Fig. 4 as the change in photocurrent as a function of the pulse area of the CROT pulse, which is in resonance with the X^0-2X^0 transition and is polarized along one of the crystal axes. A background photocurrent, linear in power, is subtracted from all data. (a) The measurement without a prepulse shows a flat line because the input state is the QD ground state $|00\rangle$ and the CROT pulse is off-resonant, as in Fig. 2(a). For two-color measurements, a prepulse—also polarized along one of the crystal axes—precedes the CROT pulse, preparing an exciton state. (b) In the measurement with cross polarized pulses, an exciton is prepared polarized

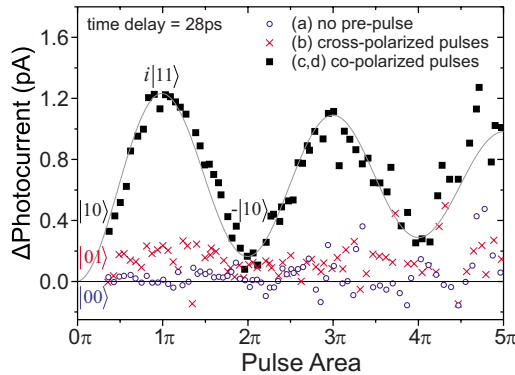


FIG. 4. (Color online) Conditional exciton-biexciton (X^0-2X^0) Rabi rotation (change in photocurrent vs pulse area for a pulse in resonance with the X^0-2X^0 transition). (○) The single-pulse measurement shows no oscillation as the pulse is off-resonant, as in Fig. 2(a). For two-pulse measurements, a linearly polarized preparation pulse prepares the X^0 state. (●) With copolarized pulses, a Rabi rotation between the X^0 and $2X^0$ states is observed [corresponding to Figs. 2(c) and 2(d) for pulse areas of π and 2π , respectively]. (×) Polarization selection rules suppress the Rabi rotation for cross polarized pulses, as in Fig. 2(b). The corresponding logic states are indicated.

TABLE I. Calculated truth table for the CROT gate.

Out\in	00	01	10	11
00	1	0.12	0.07	0.05
01	0	0.88	0.04	0.06
10	0	0	0.07	0.82
11	0	0	0.82	0.07

orthogonally to the control pulse yielding an input state of $|01\rangle$. A flat response is measured as polarization selection rules suppress the X^0-2X^0 transition, as in Fig. 2(b). (c)–(d) With copolarized pulses, an exciton is prepared with the same polarization as the control pulse. The input state is then $|10\rangle$, and more than two periods of a weakly damped Rabi rotation between the $|10\rangle$ and $|11\rangle$ states are observed. This corresponds to Figs. 2(c) and 2(d) for pulse areas of π and 2π , respectively. These experiments demonstrate the truth table of the CROT gate for pure qubit input states.

The ratio of the optical dipole moments of the $0-X^0$ and X^0-2X^0 transitions can be measured using the period of the Rabi rotations. The optical dipole moments are about the same with $\frac{\mu(X^0-2X^0)}{\mu(0-X^0)} = 0.95 \pm 0.03$, which is comparable to previous studies in GaAs interface dots²⁰ where a value of 0.85 ± 0.08 was found. To achieve a π pulse, a steady-state power of $1.7 \mu\text{W}$ is incident on the device, for a Gaussian pulse with FWHM of 10 ps.

In the long term, high fidelity gates will be needed to realize fault tolerant quantum information processing. It is therefore useful to evaluate the performance of this CROT gate in an InAs dot and compare it with that of a GaAs dot.⁶ Since the potential coherence times of InAs dots are far superior to GaAs dots [600 ps (Ref. 9) versus 50 ps (Ref. 6)], much higher gate fidelities are expected. One feasible comparison is to calculate the fidelity using experimentally determined parameters in a four-level atom model as described in the supplementary information of Ref. 6. For the data presented in Fig. 4, the exciton coherence time is limited by electron tunneling to $T_2 = 130 \pm 20$ ps—giving the truth table shown in Table I—and a fidelity of 0.87 ± 0.04 compared to 0.7 for GaAs interface dots where T_2 is limited by the radiative lifetime to 46 ps.⁶

An alternative comparison is to estimate the number of operations before coherence loss. For comparison, we define a ratio \mathcal{G} of the single exciton coherence time T_2 to the gate time of the operation, defined as the full width half maximum of the control pulse T_{FWHM} . Here the ratio is $\mathcal{G}(\text{InAs}) = \frac{130 \text{ ps}}{10 \text{ ps}} = 13$, which compares favorably with the GaAs (Ref. 6) dot case $\mathcal{G}(\text{GaAs}) = \frac{46 \text{ ps}}{5 \text{ ps}} = 9.2$. Further improvements to the coherence times could be achieved by optimizing the dot size and tunnel barriers to achieve a more closely matched electron and hole tunneling rates.¹⁵ For example, if similar calculations are made using state-of-the-art values for photocurrent detection with InAs dots (laser bandwidth 0.4 meV, $T_2 = 320$ ps)⁵ a fidelity of 0.97 and $\mathcal{G} = 64$ is in prospect. We note that in the region of interest (pulse area $\Theta < 2\pi$) the model is in good agreement with the Rabi rotation data, where the signal at 2π returns to its value at 0π to within

15%. However, the model does not account for intensity damping effects²¹ and should therefore be treated cautiously. Overall, the comparison supports the expectation that much higher fidelity quantum gates are possible with InAs dots compared to GaAs dots.

V. POLARIZATION DEPENDENCE OF EXCITON-BIEXCITON RABI ROTATION

Now we examine the case of a pulse sequence with arbitrary polarization. The polarization of the control laser may be used to drive both exciton-biexciton transitions simultaneously, and by analogy with similar atomic Λ transitions,¹³ should provide an additional degree of control over the two-qubit operation. We thus present a study of the polarization properties of the exciton-biexciton Rabi rotation. We consider the case of two laser pulses, designated as (1) and (2), with carrier frequencies on-resonance with the $(0-X^0)$ and (X^0-2X^0) transitions, respectively. Both pulses are spectrally narrow so that they excite only one set of transitions. The control Hamiltonian in the rotating frame of the states $|00\rangle, |\uparrow\rangle, |\downarrow\rangle, |11\rangle$, where the spin up/down exciton states \uparrow/\downarrow are used for ease of presentation, is given by

$$\hat{H} = \frac{1}{2} \begin{bmatrix} 0 & \Omega_+^{(1)} & \Omega_-^{(1)} & 0 \\ \Omega_+^{(1)*} & 0 & \delta_{fs} & \Omega_-^{(2)} \\ \Omega_-^{(1)*} & \delta_{fs} & 0 & \Omega_+^{(2)} \\ 0 & \Omega_-^{(2)*} & \Omega_+^{(2)*} & 0 \end{bmatrix}, \quad (1)$$

where $\hbar = 1$, δ_{fs} is the fine-structure splitting, and $\Omega_{\pm}^{(\alpha)}$ are the σ_{\pm} circularly polarized components of the complex Rabi frequency of each laser. For the sake of clarity, we neglect coherence loss. If the pulses have no spectral or temporal overlap and are much shorter than the fine-structure period, the control Hamiltonian may be interpreted as a time sequence of rotations \hat{U}_{γ} .

For the prepulse the control Hamiltonian reduces to:

$$\hat{H}_1 = \frac{1}{2} |00\rangle [\Omega_+^{(1)} \langle \uparrow | + \Omega_-^{(1)} \langle \downarrow |] + \text{H.c.} \equiv \frac{\Omega_1}{2} |00\rangle \langle A_1 | + \text{H.c.} \quad (2)$$

where $\Omega_{\alpha} = \sqrt{|\Omega_+^{\alpha}|^2 + |\Omega_-^{\alpha}|^2}$ is the effective Rabi frequency of pulse (α). Here the vacuum exciton transitions form a three-level V configuration.²² The prepulse drives a Rabi rotation between the vacuum state $|00\rangle$ and the exciton spin superposition state $|A_1\rangle$ labeled as the active state, leaving the orthogonal inactive state $|\bar{A}_1\rangle$ untouched. Hence the full polarization of a prepulse with pulse area of π is imprinted on the exciton spin.

During the interpulse time interval, the fine-structure drives a rotation \hat{U}_{fs} between exciton spin-up and spin-down states.²³ For the CROT pulse the control Hamiltonian reduces to

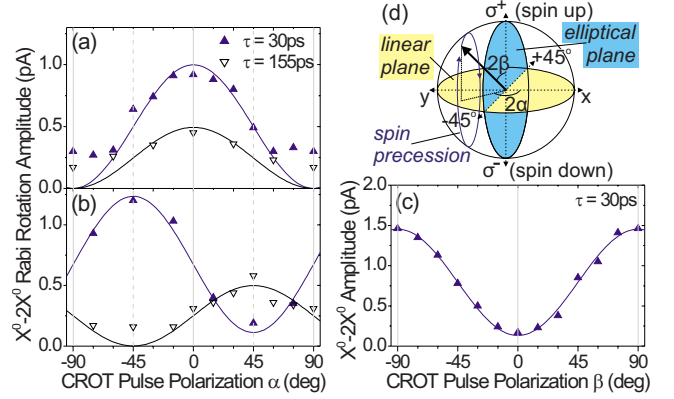


FIG. 5. (Color online) Amplitude of the X^0-2X^0 Rabi rotation measured as a function of the polarization of the CROT pulse. (a)–(b) Linearly polarized CROT pulse probes exciton created with (a) x and (b) -45° linearly polarized prepulses. (c) An elliptically polarized CROT pulse probes exciton created by σ_+ polarized prepulse. Full lines (a)–(c) are fits to data using: $\Delta PC \propto |\langle A_2 | \hat{U}_{fs} | A_1 \rangle|^2$. (d) Poincaré sphere representation of exciton spin with spin precession due to fine structure.

$$\hat{H}_2 = \frac{1}{2} [\Omega_-^{(2)} |\uparrow\rangle + \Omega_+^{(2)} |\downarrow\rangle] \langle 11 | + \text{H.c.} \equiv \frac{\Omega_2}{2} |A_2\rangle \langle 11 | + \text{H.c.} \quad (3)$$

Here the exciton-biexciton transitions form a three-level Λ configuration where the CROT pulse drives a Rabi rotation between the active exciton spin superposition state $|A_2\rangle$ and the biexciton state $|11\rangle$, leaving the inactive $|\bar{A}_2\rangle$ state untouched. In essence the polarization can select any arbitrary exciton spin as the target $|\bar{A}_2\rangle$ and control $|A_2\rangle$ qubits and this can be used as a control tool. For example, the polarization of a CROT pulse with a pulse area of π can select an exciton spin superposition to project into the biexciton state, providing a means of detecting the exciton spin. Alternatively, full optical control of the exciton spin can be achieved as follows: A CROT pulse with a pulse area of 2π imparts a detuning dependent phase shift of up to π (Refs. 16 and 24) on $|A_2\rangle$ with respect to $|\bar{A}_2\rangle$. Moreover since any exciton spin superposition may be selected as $|A_2\rangle$, full optical control of the exciton spin can be achieved using the polarization of the pulse.²² This results in a gate time limited by the duration of the control pulse far faster than two-pulse techniques where the exciton spin is controlled using the fine-structure beat.^{2,5}

To test this model, we study the dependence of the $0-X^0$ and X^0-2X^0 Rabi rotations on the polarizations of the pre and CROT pulses. Figure 5(d) shows a Poincaré sphere representation of the polarization where $(\Omega_+, \Omega_-) = \Omega(e^{i\alpha} \cos \beta, e^{-i\alpha} \sin \beta)$. The period of the $0-X^0$ and X^0-2X^0 Rabi rotations are independent of polarization. For time resolved measurements (not shown), where both the pre and CROT pulses are π pulses, fine-structure beats with a period of 320 ps are observed. To test that the CROT pulse drives a Rabi rotation between the “active” exciton spin superposition $|A_2\rangle$ and the biexciton $|11\rangle$ states, we measure the amplitude of the Rabi rotation as a function of the polariza-

tion of the CROT pulse in both the linear and elliptical planes of the Poincaré sphere [Fig. 5(d)], and compare it with the model: $\Delta PC \propto |\langle A_2 | \hat{U}_{fs} | A_1 \rangle|^2$.

(*Linear plane*) The prepulse is linearly polarized along the x axis to excite an energy eigenstate, and the Rabi rotations are measured as a function of linear polarization α_{crot} with ($\alpha_{\text{pre}}=0, \beta_{\text{pre}}=\beta_{\text{CROT}}=+45^\circ$). Figure 5(a) presents the results. A cosine dependence is observed where maximum signal occurs when the pulses are colinearly polarized. This is true for all time delays since there is no precession of the exciton spin. Next, for the results presented in Fig. 5(b), a -45° linearly polarized prepulse is used and the amplitude recorded as a function of the CROT linear polarization ($\alpha_{\text{pre}}=-45^\circ, \beta_{\text{pre}}=\beta_{\text{CROT}}=+45^\circ$). At short time delay ($\delta_{fs}\tau < \pi/2$) maximum signal again occurs for colinearly polarized excitation. However, at $\tau=155$ ps the maximum now occurs for cross linear polarization due to the fine-structure rotation and the amplitude is reduced due to electron tunneling. In Figs. 5(a)–5(c) the solid lines show the good fits to data using $\Delta PC \propto |\langle A_2 | \hat{U}_{fs} | A_1 \rangle|^2$, where the amplitudes of the oscillations are the only fitting parameters.

(*Elliptical plane*) To probe the elliptically polarized plane, a circularly polarized prepulse is used ($\alpha_{\text{pre}}=\alpha_{\text{crot}}=45^\circ, \beta_{\text{pre}}=0$) and the amplitude of the Rabi rotation measured as a function of the ellipticity angle of the CROT pulse β_{CROT} . At short time delay, the maximum is observed for cross circular excitation [see Fig. 5(c)]. The measurements show a close agreement with the model for both planes of the Poincaré sphere, implying that the full polarization of the prepulse is stored in the exciton spin and then a selected

component is projected into the biexciton state by the CROT pulse. This further implies that the polarization of the CROT pulse selects an exciton spin superposition to couple optically to the biexciton state.

VI. CONCLUSIONS

In conclusion, we have demonstrated a CROT quantum-logic gate for two excitonic qubits in a single InGaAs/GaAs dot with a high fidelity of 0.87 ± 0.04 . This extends the work of Li *et al.*⁶ from a GaAs interface dot to InGaAs/GaAs self-assembled dot systems. Such self-assembled dots possess longer coherence times paving the way to potential gate fidelities in excess of 0.95 in optimized structures. This system also offers the potential for scalability as a result of the formation of vertically and laterally coupled dots under appropriate growth conditions. Furthermore, we find that the polarization of the control pulse may be used to select arbitrary exciton spin superpositions as the target and control qubits. This property may be used to compile an operator, which combines elements of the CROT and bit swap operations into a single control pulse offering a more efficient control sequence than a series of CROT and single qubit operations.

ACKNOWLEDGMENTS

This work was funded by EPSRC-GB (UK) under Grant No. GR/S76076 and the QIPIRC U.K.

*s.boyle@shef.ac.uk

[†]a.j.ramsay@shef.ac.uk

¹A. Barenco, D. Deutsch, A. Ekert, and R. Jozsa, Phys. Rev. Lett. **74**, 4083 (1995).

²N. H. Bonadeo, J. Erland, D. Gammon, D. Park, D. S. Katzer, and D. G. Steel, Science **282**, 1470 (1998).

³A. Zrenner, E. Beham, S. Stuffer, F. Findeis, M. Bichler, and G. Abstreiter, Nature (London) **418**, 612 (2002).

⁴T. H. Stievater, Xiaoquin Li, D. G. Steel, D. Gammon, D. S. Katzer, D. Park, C. Piermarocchi, and L. J. Sham, Phys. Rev. Lett. **87**, 133603 (2001).

⁵S. Stuffer, P. Ester, A. Zrenner, and M. Bichler, Phys. Rev. B **72**, 121301(R) (2005).

⁶X. Li, Y. Wu, D. G. Steel, D. Gammon, T. H. Stievater, D. S. Katzer, D. Park, C. Piermarocchi, and L. J. Sham, Science **301**, 809 (2003).

⁷E. Biolatti, R. C. Iotti, P. Zanardi, and F. Rossi, Phys. Rev. Lett. **85**, 5647 (2000).

⁸F. Troiani, U. Hohenester, and E. Molinari, Phys. Rev. B **62**, R2263 (2000).

⁹P. Borri, W. Langbein, S. Schneider, U. Woggon, R. L. Sellin, D. Ouyang, and D. Bimberg, Phys. Rev. Lett. **87**, 157401 (2001).

¹⁰H. J. Krenner, M. Sabathil, E. C. Clark, A. Kress, D. Schuh, M. Bichler, G. Abstreiter, and J. J. Finley, Phys. Rev. Lett. **94**, 057402 (2005).

¹¹E. A. Stinaff, M. Scheibner, A. S. Bracker, I. V. Ponomarev, V. L. Koronev, M. E. Ware, M. F. Doty, T. L. Reinecke, and D. Gammon, Science **311**, 632 (2006).

¹²H. Heidemeyer, U. Denker, C. Müller, and O. G. Schmidt, Phys. Rev. Lett. **91**, 196103 (2003).

¹³P. Král, I. Thanopoulos, and M. Shapiro, Rev. Mod. Phys. **79**, 53 (2007).

¹⁴A. M. Weiner, Rev. Sci. Instrum. **71**, 1929 (2000).

¹⁵R. S. Kolodka, A. J. Ramsay, J. Skiba-Szymanska, P. W. Fry, H. Y. Liu, A. M. Fox, and M. S. Skolnick, Phys. Rev. B **75**, 193306 (2007).

¹⁶A. J. Ramsay, S. J. Boyle, R. S. Kolodka, J. B. B. Oliveira, J. Skiba-Szymanska, H. Y. Liu, M. Hopkinson, A. M. Fox, and M. S. Skolnick, Phys. Rev. Lett. **100**, 197401 (2008).

¹⁷S. Stuffer, P. Machnikowski, P. Ester, M. Bichler, V. M. Axt, T. Kuhn, and A. Zrenner, Phys. Rev. B **73**, 125304 (2006).

¹⁸We attribute the different signals of dots B and C for co/cross polarized excitation in Fig. 3 to mechanical drift of the setup. The signal is optimized for dot A, resulting in a robust signal, whereas the unoptimized signals of peaks B and C are more sensitive to changes in the setup. All possible transitions: $0-X^0$, $0-2X^0$, X^0-2X^0 , and $h-X^+$ associated with dot A have been identified. Under resonant excitation peaks B and C, show a $0-X^0$ like Rabi rotation, as do peaks observed in other apertures. These Rabi rotations have longer periods due to inefficient dot

laser coupling, which we attribute to the relative position of dots B and C, with respect to the aperture. Similar features in other apertures are randomly distributed in energy with respect to the stronger peaks, further underlining their identity as separate dots.

- ¹⁹The photocurrent detection efficiency is limited by the hole tunneling rate as shown in Ref. 15. Hence the X^0-2X^0 signal, which involves tunneling of two holes, is weaker than the $0-X^0$ signal at this bias.
- ²⁰T. H. Stievater, X. Li, D. G. Steel, D. Gammon, D. S. Katzer, and D. Park, Phys. Rev. B **65**, 205319 (2002).
- ²¹Q. Q. Wang, A. Muller, P. Bianucci, E. Rossi, Q. K. Xue, T.

Takagahara, C. Piermarocchi, A. H. MacDonald, and C. K. Shih, Phys. Rev. B **72**, 035306 (2005).

- ²²Q. Q. Wang, A. Muller, M. T. Cheng, H. J. Zhou, P. Bianucci, and C. K. Shih, Phys. Rev. Lett. **95**, 187404 (2005). In this work, an exciton spin flip was demonstrated using a 2π -pulse to drive both vacuum exciton transitions.
- ²³A. I. Tartakovskii, J. Cahill, M. N. Makhonin, D. M. Whittaker, J.-P. R. Wells, A. M. Fox, D. J. Mowbray, M. S. Skolnick, K. M. Groom, M. J. Steer, and M. Hopkinson, Phys. Rev. Lett. **93**, 057401 (2004).
- ²⁴S. E. Economou and T. L. Reinecke, Phys. Rev. Lett. **99**, 217401 (2007).